Artificial Intelligence and Human-Computer Interaction
Y. Ye and P. Siarry (Eds.)

doi:10.3233/FAIA240137

A Novel LED Spherical Visual Display System and Its Image Geometric Correction Method

Yixiong ZENG[1], Jianxi DAI, Bo XU and Kun QIU
School of Information and Communication Engineering, University of Electronic Science and Technology of China, Chengdu, China 610054

Abstract. Visual display systems have wide-ranging applications in training simulators, serving as comprehensive systems that expand the display field of view by seamlessly combining multiple display units. This paper introduces an innovative spherical display system based on LED technology, designed to achieve close-proximity real-image display within a spherical enclosure. Additionally, we propose a channel division method tailored for this novel LED spherical display to enable efficient display driving. To address geometric distortion issues that arise when rendering flat graphics on a spherical surface, we present a geometric correction method specially designed for LED spherical displays, providing a comprehensive explanation of its theoretical principles and correction process. Experimental results demonstrate that with the implementation of our proposed channel division and geometric correction methods, the number of driving channels for the LED spherical display is reduced, image cropping is minimized, and there is no need for image fusion processing. Corrected images exhibit no distortion, and channel alignment remains continuous without any displacement. This method offers a straightforward operation, requires minimal parameter settings, and is easily implementable, providing a solid foundation for the widespread application of LED spherical vision display systems the future.

Keywords. Training Simulator, visual display systems, LED spherical display, geometric correction

1. Introduction

In the realm of training simulators, visual display systems play a pivotal role as a critical component, exerting profound influence on the overall performance of simulation and the effectiveness of training outcomes. Their primary function is the real-time presentation of computationally generated virtual environments, immersing users in an environment that aims to provide a heightened level of realism in terms of visual experience [1]. Consequently, the performance of visual display systems not only directly impacts the holistic effectiveness of training simulators but also determines the quality of training outcomes attainable by the users.

The evolution of visual display systems has witnessed a progression from initial CRT monitors to liquid crystal displays (LCDs) and, most recently, to projection-based displays [2-4]. These advancements have expanded the field of view, improved display

[1] Corresponding Author: Yixiong Zeng, zyxiong@std.uestc.edu.cn

clarity, and enhanced brightness and contrast, thereby significantly augmenting the immersive qualities of visual displays. In sum, visual display systems have continually advanced and innovated in the pursuit of expanding field of view, high-definition imagery, enhanced brightness and contrast, prolonged longevity, and heightened reliability.

Presently, the domain of training simulators predominantly relies on multi-channel spherical visual display systems based on projection technology [5,6]. These systems exhibit high levels of technical maturity, characterized by their straightforward optical pathways, the realization of extensive fields of view, and the provision of high-definition displays. However, these systems remain beset with issues such as low display brightness, insufficient contrast, complex image processing, and challenging post-maintenance. These issues have served as the focal point of sustained research efforts among scientists and engineers. It is within this context that we propose a novel spherical visual display system based on Light Emitting Diode (LED) technology to address these challenges.

As LED technology continues to progress, LED pixel sizes and spacing have diminished, facilitating the development of high-density LED displays suitable for close-range viewing [7,8]. Furthermore, LED technology, as an active display technology, offers advantages in terms of high display brightness and contrast [9,10]. Consequently, the adoption of LED technology in spherical visual display systems presents several advantages, including a broad field of view, high-definition display, elevated brightness and contrast, uniform display characteristics, extended longevity, and heightened reliability. Nonetheless, the incorporation of LED technology into the domain of simulation and training still poses numerous challenges and complexities. These include achieving high-density spherical displays, LED sphere display driving and image processing, low-latency transmission for real-time display in training scenarios, ensuring consistency in LED sphere display output, and effectively addressing issues related to heat dissipation and maintenance. This paper's focal point revolves around the study of LED sphere display driving and the resolution of nonlinear distortion issues encountered in the driving process, ultimately enabling the spherical presentation of virtual visual scenes generated by front-end simulation computers.

2. LED-based spherical visual display technology

2.1. Channel partitioning and field of view design

In the context of training simulators, a key component of the visual display system is a spherical screen with a certain display radius, high resolution, and a wide field of view. Consider a display with a diameter of 7000mm, a horizontal field of view of 360°, and a vertical field of view of 130° (comprising an upper field of 90° and a lower field of 40°). The display's spatial resolution is not greater than 2 arcminutes per pixel. Calculations show that the displayed image resolution far exceeds the maximum output resolution of a single computer. Therefore, multiple image stitching is required to drive the entire spherical screen, and the screen needs to be divided into regions for effective control.

This paper proposes an approach to divide the spherical screen into 7 regions using a latitude and longitude division method, as illustrated in Figure 1. This division method offers several advantages: it facilitates LED panel production and spherical stitching, involves the least number of divided regions, and simplifies display control. Importantly, it avoids issues related to jagged stitching edges and visible seams inherent in other methods like soccer ball models or Goldberg Polyhedron [11] divisions.

The divided side regions are denoted as Channels 1 to 6, while the top region is identified as Channel 7. To ensure that each channel achieves a higher pixel utilization rate during display, we designed the maximum pixel dimensions for the side channels to be 2160 (W) × 3840 (H) points. Based on the spherical screen's radius and field of view parameters, we calculated the LED spacing to be 1.696mm. The side channels have a field of view of 60° (FovX) × 106.67° (FovY), while the top channel has a field of view of 46.66° (FovX) × 46.66° (FovY), corresponding to a maximum pixel configuration of 1680 (W) × 1680 (H) points, as depicted in Figure 1.

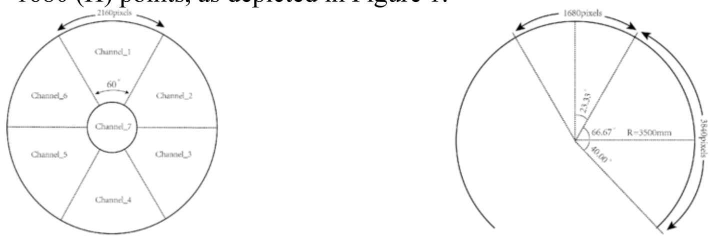

(a) (b)

Figure 1. Channel division and field of view distribution schematic. (a) Top view of the spherical display; (b) Side view of the spherical display.

It is easy to understand that when a spherical image is unfolded into a flat plane, distortion occurs. Similarly, if a flat image generated by a simulation computer is displayed on a spherical screen, distortion, known as non-linear distortion, occurs. Therefore, geometric correction is essential during the process of driving a spherical screen to ensure the proper display of images. To facilitate understanding and design, we unfold the segmented LED spherical screen onto a two-dimensional plane, as illustrated in Figure 2. It can be observed from the figure that the division method proposed in this paper actually only involves two distinct states. This is because the side channels have identical field of view ranges and pixel distributions with no overlap between channels. Consequently, geometric correction needs to be performed separately for the top channel and one of the side channels. This approach simplifies image processing and display control implementation.

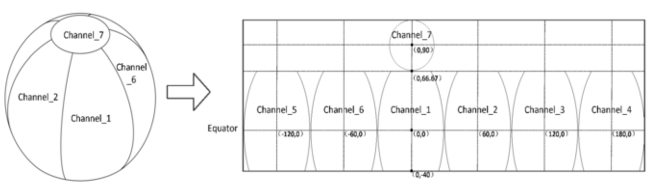

Figure 2. Spherical display channel two-dimensional field of view unfolded diagram.

2.2. System driver design

The video source for the LED spherical screen display originates from virtual simulated scenes generated by simulation computers. As outlined in the previously discussed channel division of the spherical screen, it becomes evident that the LED spherical screen necessitates the real-time generation and output of seven video streams, each boasting a resolution of 3840(W)×2160(H), in order to encompass the entirety of the LED spherical screen. Acknowledging the current hardware capabilities for image processing, a geometric correction system featuring seven channels has been devised to address the issue of non-linear distortion that occurs when mapping flat images onto the spherical screen. The precise architectural arrangement of this system is graphically illustrated in Figure 3.

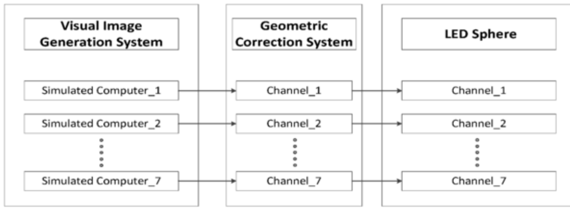

Figure 3. LED spherical display driver architecture diagram.

The geometric correction system primarily adjusts the content of the images output by the simulation computers. After the correction process, the images are also output at a resolution of 3840(W)×2160(H) to the LED sphere. Referring to the unfolded diagram in Figure 2, the LED sphere's top section is directly driven for display by capturing circular images at a resolution of 1680(W)×1680(H). On the other hand, for the side sections, a two-step approach involving a 90° rotation followed by image compression is used to achieve a one-to-one mapping between the LED in the side channels and the image pixels. This process ultimately enables the complete driving display of the entire LED spherical display system.

3. Proposed method of geometric correction

In the context of the image generation system based on camera models for real-time visual scene rendering, the geometric correction process of the LED spherical display involves establishing a mathematical model that encompasses a virtual camera, the LED spherical display, and the viewpoint. This model is used to determine the mapping relationship between the projection plane of the area to be corrected and the spherical surface. The objective is to display planar images on the spherical surface without distortion or aberration. As per the channel division method proposed in this paper, the geometric correction process involves only the side and top sections.

3.1. Geometric correction for side channel

Given that the side of the LED spherical display is divided into six identical channels, the correction methods and parameters for each channel are entirely the same. Taking a single channel as an example, it has a horizontal field of view of 60°, a vertical downward field of view of 40°, and an upward field of view of 66.67°. Assuming a point P on the spherical surface is projected onto the plane to obtain point P', geometric correction involves establishing the mapping relationship between point P and P'.

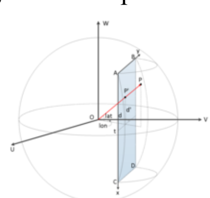

Figure 4. Geometric correction principle diagram for side channel.

As shown in Figure 4, we establish a spherical coordinate system and a projection plane coordinate system. Assuming the distance from the projection plane to the sphere's center is d, we can derive the x coordinate of point P' as follows:

$$\begin{cases} x = t - d' \\ d' = d / \cos(lon) \cdot \tan(lat) \end{cases} \tag{1}$$

From formula (1), we can easily analyze that on the sphere, lines of equal latitude, influenced by $\cos(lon)$, result in a decrease in x as lon increases. Consequently, lines of the same latitude are mapped onto the plane as concave lines with high sides and a low middle, which is the main characteristic of the flat graphics output by the visual image generation system. Our geometric correction is a "convex" operation to restore the image.

Considering that the projection in the equatorial region does not deform, and the number of pixels in the equatorial region of the system is known, specifically 2160 pixels, we can calculate the values of t and d from formula (1) as follows:

$$\begin{cases} t = C \cdot (\tan(N) / (\tan(N) + \tan(S))) \\ d = t \cdot (\cos(E) / \tan(N)) \end{cases} \tag{2}$$

Where N is the maximum vertical upper viewing angle for the side channels, S is the maximum vertical lower viewing angle, E represents half of the maximum horizontal viewing angle, and C represents the number of image pixels on the equator. Substituting Equation 2 into Equation 1 gives the mapping relationship of x between the sphere and the projection plane.

Due to the special nature of the LED spherical display's side channels, when calculating the y coordinate of P', the deformation of the meridians can be nearly ignored, and since the pixels on the meridians are not lost, it can be assumed that the y pixels do not change. Therefore, the geometric correction for the side channels only needs to consider the mapping relationship of the x coordinate.

3.2. Geometric correction for top channel

The top channel, unlike the side channels, has a projection plane that forms a perfect circle. Therefore, both x and y coordinates mapping need to be considered. For this channel, the horizontal field of view and vertical field of view are both equal to 46.66°, with a corresponding maximum image pixel count of 1680 points. We aim to determine the mapping relationship of a point Q on the sphere projecting onto the point Q' on the plane.

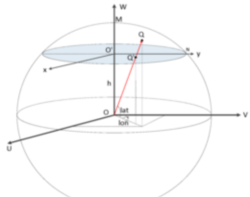

Figure 5. Geometric correction principle diagram for top channel.

As illustrated in Figure 5, we establish a spherical coordinate system and a projection plane coordinate system. Assuming that the distance from the sphere's center to the projection plane is h, we can calculate the x and y coordinates of point Q' as follows:

$$\begin{cases} x = h \cdot \cot(lat) \cdot \sin(lon) \\ y = h \cdot \cot(lat) \cdot \cos(lon) \end{cases} \tag{3}$$

Similarly, we can determine the y and v coordinates of point Q on the sphere as:

$$\begin{cases} u = R \cdot \cos(lat) \cdot \cos(lon) \\ v = R \cdot \cos(lat) \cdot \sin(lon) \end{cases} \tag{4}$$

Where R represents the radius of the spherical display. Because both h and R are constants, the positions of points on the spherical surface (Q) and the projection plane (Q') are exclusively determined by the latitudinal lat and longitudinal lan angles. This fundamental relationship establishes the mapping between these two points. It is evident that as one approaches the polar regions of the spherical display, the disparity between the spherical surface and the projection plane diminishes. Consequently, if the field of view for the top channel of the LED spherical display system is intentionally designed to be smaller, it becomes feasible to employ uncorrected images in place of the geometrically corrected ones. This strategic choice holds significant advantages, particularly during the subsequent phases of hardware implementation, where the demand for real-time processing and display is paramount in ensuring system efficiency.

4. Experimental results

To validate the correctness of the algorithm proposed in this paper, we initially conducted simulations using Matlab software to confirm the algorithm's rationality. Subsequently, we implemented the algorithm into the hardware of the geometric correction system and conducted tests on an LED spherical display. Therefore, during the algorithm simulation, we employed 3DMAX software to simulate the visual image generation system for generating test images. The process involved setting up a 3D sphere model and placing a virtual camera at the sphere's center. The virtual camera captured the spherical images corresponding to the field of view angles divided by channels of the LED spherical display. This process resulted in the generation of high-resolution images at 3840 (W) × 2160 (H), matching the image depicted in Figure 1, which served as the pre-geometric correction test image. After subjecting the images to the algorithm, we obtained the post-correction simulation images.

Figure 6 illustrates a before-and-after comparison of side channel correction, where (a) represents the image before correction. It can be observed that the image exhibits distortion, with lines of latitude diverging from the equator (indicated by the red line) towards the equatorial region, and uneven spacing between lines of latitude. The equatorial region has smaller spacing, while the spacing increases towards the polar regions. Notably, the lines of longitude exhibit minimal variation, and this behavior is determined by the LED spherical display and the channel division method proposed in this paper. In contrast, (b) represents the image after correction, where it is evident that the lines of latitude and longitude are undistorted, evenly distributed, and equally spaced. Therefore, during LED display driving, based on the principle of row-by-row scanning, it is clear that after correction, images from the same row can be mapped to LEDs at the same latitude on the spherical surface, and images from the same column can be mapped to LEDs at the same longitude on the sphere. This ensures that the spherical surface displays visual scene images without any form of distortion after correction. If the spacing between the white lines in the image represents a 5° angle, it can be confirmed that the field of view angle depicted in the images remains unchanged before and after correction, thus validating that the algorithm proposed in this paper ensures distortion-free image correction.

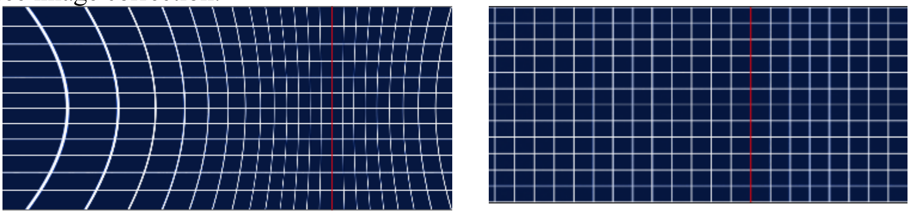

(a) (b)

Figure 6. Geometric correction before and after simulation images (side). (a) before calibration; (b) after calibration.

Figure 7 illustrates a comparison between the pre-correction and post-correction images for the top channel. Unlike the side channels, the image in this case appears as a circular representation, with each concentric circle denoting the same latitude. Due to the smaller size of the top region, the changes before and after correction are relatively minor. If the spacing between the white concentric circles is set at 5°, it can be verified that the field of view for the top channel remains unchanged before and after correction. Consequently, this also confirms that the top channel exhibits distortion-free and lossless images after correction.

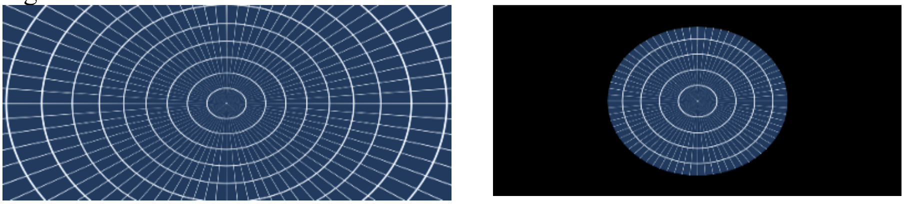

(a) (b)

Figure 7. Geometric correction before and after simulation images (top). (a) before calibration; (b) after calibration.

To further validate the correctness of this geometric correction method, we set up a real LED spherical visual display system. Firstly, we configured the images to be displayed based on the field of view parameters of the LED spherical display. Subsequently, we implemented the algorithm proposed in this paper into the hardware of the geometric correction system and compared the image states before and after correction. As shown in Figure 8, it presents the lines of latitude and longitude displayed on two channels of the LED spherical display. Figures (a) and (b) represent the actual LED spherical display images with and without correction, respectively. From Figure (a), it is evident that the lines of latitude, which should correspond to the same latitude, are not aligned on the actual LED spherical display. Within each channel, the lines of latitude is severely distorted, and there are discontinuities between channels. This illustrates that displaying images without correction leads to even more severe distortions. In contrast, Figure (b) demonstrates that both within and between channels, the lines representing the same latitude are neither distorted nor discontinuous. If one were to measure the longitude and latitude of each line using a total station at the center of the sphere, it would become apparent that each line maintains consistent longitude and latitude. This further confirms that, after being processed using the geometric correction method proposed in this paper, the displayed images are free from distortion and loss.

(a) (b)

Figure 8. Before and after geometric correction latitude and longitude lines diagram. (a) uncorrected image; (b) corrected image.

(a) (b)

Figure 9. Visual scene images before and after geometric correction. (a) Comparison images before and after geometric correction for two channels; (b) Images after geometric correction for two channels.

Figure 9 further demonstrates the disparities in displaying virtual scenes on the LED spherical display before and after correction. The experiment utilizes two channels, as depicted in Figure (a), with the left channel representing the uncorrected image and the right channel representing the corrected image. In virtual scenes of this kind, the end of the runway typically corresponds to the equator line, aligning with the center of the LED spherical display. It is quite evident that in the uncorrected image, the runway appears lower and cannot align with the corrected image. Figure (b) showcases the results after applying correction to both channels. Not only are the images perfectly aligned, but details such as numbers on the runway are also discernible. If measured with a theodolite, it can be confirmed that the end of the runway aligns horizontally with the sphere's center.

Figure 10 demonstrates a commonly used method to verify the proper display of the spherical screen. In this approach, a 3D spherical model is generated within the scene image generation system. The model includes not only the scene image but also evenly spaced lines of latitude and longitude (typically set at 5° intervals). Similar to the previous description, the spherical model is segmented into multiple channels, each outputting images at a resolution of 3840×2160. From Figure 10, it is evident that the lines of latitude and longitude in the scene are uniformly distributed and continuous, without bending or distortion, and the image remains intact. This further substantiates the feasibility of the LED spherical screen channel division proposed in this paper and the correctness of the geometric correction.

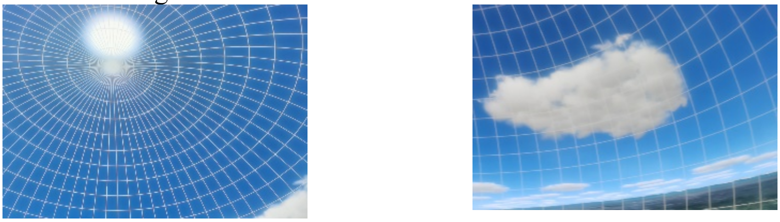

(a) (b)

Figure 10. Visual scene images after geometric correction. (a) Image of top;(b) Image of side.

5. Conclusions

In order to enhance the display performance of the visual scene display system in simulation trainers, we have introduced a novel LED spherical visual display system. Compared to traditional LCD panel arrays and projection-based spherical displays, it offers numerous advantages, including higher display brightness, contrast, a larger field of view, and improved clarity, resulting in a more realistic visual experience. This paper focuses on the pivotal issue of driving the LED spherical display and presents an LED spherical display channel division method along with an efficient geometric correction approach. This ensures that the LED spherical display can not only present spherical images accurately but also maintain the original visual quality of the images. When compared to traditional projection-based spherical displays for achieving the same spherical display system, our approach offers fewer channels and higher pixel utilization, leading to cost savings and superior performance. This provides a more advanced, realistic, and cost-effective solution for visual scene display in simulation trainers, with significant potential applications.

Acknowledgments

This work was supported by National Natural Science Foundation of China (U22A2086) and the Fundamental Research Funds for the Central Universities (ZYGX2020ZB043).

References

[1] Baarspul M. A review of flight simulation techniques. Prog. Aerosp. Sci. 1990; 27(1): 1-120. doi: 10.1016/0376-0421(90)90006-6.
[2] Lantz E. Future directions in visual display systems. ACM SIGGRAPH Comput. Grap. 1997; 31(2): 38-42. doi: 10.1145/271283.271301.
[3] Song M, Park S, Kang Y. A survey on projector-based PC cluster distributed large screen displays and shader technologies. In: CGVR. 2007; 153-159. doi: 10.1007/978-3-540-74873-1_57.
[4] Miljković D. Wide-view visual systems for flight simulation. MIPRO .2009.
[5] Ma B, Lin L, Ma QY. Design and optimization for ellipsoid back projection screen of collimated display system in flight simulator. In: Proc. AsiaSim. 2008; 1446-1450. doi:10.1109/ASC-ICSC.2008.4675602.
[6] Wang X, Yan K, Liu Y. Automatic geometry calibration for multi-projector display systems with arbitrary continuous curved surfaces. IET Image Process. 2019; 13(7): 1050-1055. doi:10.1049/iet-ipr.2018.5575.
[7] Huang Y, Tan G, Gou F, Li MC, Lee SL, Wu ST. Prospects and challenges of mini-LED and micro-LED displays. J. Soc. Inf. Display. 2019; 27(7): 387-401. doi: 10.1002/jsid.760.
[8] Tripathi A, et al. A conformable active matrix LED display. In: International Meeting on Information Displays. In Proc. Int. Meet. Inf. Displays. 2015.
[9] Huang Y, Hsiang EL, Deng MY, et al. Mini-LED, Micro-LED and OLED displays: present status and future perspectives. Light Sci Appl. 2020; 9: 105. doi: 10.1038/s41377-020-0341-9.
[10] Zhang H, Tu S, Li L, et al. Large scale transparency-adjustable mini-LED display with recoverable color gamut by a highly transparent electrochromic shutter. Opt. Express. 2022; 30: 39904-39910. doi: 10.1364/OE.469659.
[11] Schein S, Gayed JM. Fourth class of convex equilateral polyhedron with polyhedral symmetry related to fullerenes and viruses. Pro. Nati. Acad. Sci. 2014; 111(8): 2920-2925. doi: 10.1073/pnas.1310939111.